



Vacancy diffusion and its consequences for void growth at the interface of a stripping metal electrode and solid electrolyte

S.S. Shishvan^{b,a}, N.A. Fleck^a, R.M. McMeeking^{c,d,e}, V.S. Deshpande^{a,*}

^a Department of Engineering, University of Cambridge, Cambridge CB2 1PZ, UK

^b Department of Structural Engineering, University of Tabriz, Tabriz, Iran

^c Departments of Materials and Mechanical Engineering, University of California, Santa Barbara CA 93106, USA

^d School of Engineering, University of Aberdeen, King's College, Aberdeen AB24 3UE, UK

^e INM-Leibniz Institute for New Materials, Campus D2 2, Saarbrücken 66123, Germany

ARTICLE INFO

Keywords:

Solid-state battery

Ceramic electrolyte

Butler-volmer kinetics

Void growth

ABSTRACT

It is commonly observed that voids can nucleate and grow in the lithium anode of a solid state Li-ion battery at a location adjacent to the solid electrolyte during the stripping (discharge) phase of the battery; a similar phenomenon is observed in sodium-based batteries. It is hypothesised in the current literature that the formation of these voids is due to the coalescence of vacancies that have been generated at the electrode/electrolyte interface when metal atoms are oxidized and transported into the electrolyte: the slow diffusion of the vacancies away from the electrolyte interface into the adjacent electrode results in their coalescence and the consequent growth of voids. These hypotheses are challenged in the current study by using the Onsager formalism to generate a variational principle for vacancy diffusion. Our analysis reveals that no driving force exists for the diffusion of vacancies into a homogeneous metal electrode that thins by stripping. This finding is contrary to models in the literature which have mistakenly assumed that the vanishing flux at the current collector prevents rigid body motion (drift) of the electrode which in turn prevents thinning of the electrode during stripping. Based on our analysis, we conclude that vacancy diffusion within a homogeneous electrode is not responsible for the nucleation and growth of voids at the interface between a stripping metal electrode and a solid electrolyte.

1. Introduction

Lithium metal is attractive for use as the negative electrode, commonly known as the anode, for Li-ion batteries due to the high energy density of lithium oxidation [1,2]. Lithium dendrites grow in liquid electrolytes at a fast rate of battery charge [3,4] and this has led to the use of solid electrolytes for dendrite suppression [5]. However, dendrites, which are also referred to as Li filaments [6] in solid electrolytes, still grow in polymer [7] and ceramic [8] electrolytes. This has been supported by a large body of recent experimental work on Li and Na cells with ceramic electrolytes reported by the groups of Bruce [9–11], Sakamoto [6,12–14] and Shearing [15,16]. Bruce and co-workers [9,10] have also observed that voids form in the Li metal electrode during stripping of the electrode. These voids form at the interface between the electrode and solid electrolyte and increase the electrode/electrolyte interface resistance to level that makes the battery unviable. Moreover, both observations [9,17] and simulations [18,19] suggest that Li

filaments grow preferentially in the vicinity of these voids and that the presence of these voids also lowers the critical current density for short-circuiting of the cell due to filament growth. Thus, an understanding of void nucleation and growth at the metal electrode/solid electrolyte interface during stripping is essential. This has spurred a large experimental activity on the nucleation and growth of these voids in Li [20–23] and Na [9,10] electrodes; see Fig. 1 for an example of scanning electron microscope (SEM) images of voids in Li electrodes.

Numerous modelling studies have attempted to develop an understanding of the growth of these voids. In broad terms, these studies assume that void growth occurs either (i) by creep deformation of the metal [24–28] or (ii) by the generation of vacancies in the metal at the electrode/electrolyte interface. In the latter treatments, these vacancies are said to diffuse into the electrode or coalesce at the interface to form macroscopic voids [20,21]. A few studies [23,29,30] have combined both the creep deformation and the vacancy flux mechanisms, see the recent review [31] for further details. Here, we begin by discussing these

* Corresponding author.

E-mail address: vsd20@cam.ac.uk (V.S. Deshpande).

<https://doi.org/10.1016/j.electacta.2023.143081>

Received 12 June 2023; Received in revised form 21 August 2023; Accepted 23 August 2023

Available online 25 August 2023

0013-4686/© 2023 The Author(s). Published by Elsevier Ltd. This is an open access article under the CC BY license (<http://creativecommons.org/licenses/by/4.0/>).

two mechanisms to give our current study the appropriate context.

The studies modelling void growth by creep envision that a pre-existing defect such as a void/impurity particle is present on the electrode/electrolyte interface. This impurity gives rise to flux focussing over the periphery of the defect [24–26]. The associated creep flow within the metal electrode then results in growth of a void around the initial defect. Given that the electrode/electrolyte interface is fixed in space, Shishvan et al. [24] used a coupled fluid Eulerian/electrochemical analysis to investigate this mechanism. However, their calculations demonstrated that standard Butler-Volmer kinetics leads to insufficient flux focussing for void growth to occur. Roy et al. [25] performed simpler decoupled calculations of essentially the same problem. However, they used a Lagrangian method to model the creep of the electrode but added in the translation (that is, drift) of the electrode associated with the thinning of the stripping electrode as a post-processing step and came to the same conclusion as that of Shishvan et al. [24]: the flux focussing associated with Butler-Volmer kinetics is insufficient to cause void growth. Shishvan et al. [24] further suggested that creep of the metal (Li) modifies the interface kinetics and thereby increases flux focussing. Agier et al. [26] used this idea to compute the growth of a void around an impurity particle on the electrode/electrolyte interface. However, their calculations show that voids initially form and grow but ultimately collapse due to a combination of the electrode drift (thinning) and creep.

Other models attribute the formation and growth of voids to the diffusion of vacancies within the electrode [20,21]. In these models, it is hypothesised that vacancies are generated at the interface when metal atoms are oxidized and transported into the electrolyte. These vacancies then diffuse away from the interface, with the counter-motion of metal atoms allowing stripping to continue; see Fig. 2a. Thus, so long as the diffusion of vacancies is sufficiently fast to replenish the metal atoms stripped from the electrode there is no vacancy build-up at the interface. Above a critical stripping current, vacancies are generated at the interface at a faster rate than diffusion can replenish them implying that the build-up and subsequent congregation of these vacancies result in the formation of the observed macroscopic voids. The models to support this physical picture either write down empirical diffusion relations [20,21, 23,29] or solve detailed field equations [30]. They predict that cell failure can occur due to vacancy accumulation and/or void formation at the electrode/electrolyte interface. However, all these models miss a critical aspect of the physics. During stripping, there may or may not be vacancy diffusion within the electrode but there exists clear evidence that the electrode thins as metal is transported from the stripping to the plating electrode through the electrolyte (Fig. 2b). The vacancy diffusion analyses reported in the literature [20,21,23,29,30] neglect this thinning or drift of the electrode; in contrast, this drift was accounted for in the creep models [24–26] as mentioned above. Vacancies formed at the electrode/electrolyte interface by the stripping of the metal (Fig. 2b) can be annihilated by electrode drift; by neglecting this contribution from drift, the models are missing a key physics that might fundamentally change the conclusion on the significance of vacancy diffusion. In addition, these models also seem to ignore the energetic barrier for vacancies to coalesce to form voids in Li. For example, the enthalpy

of vacancy formation in Li is $\sim 50\text{kJ mol}^{-1}$ [32] but this energy rises to $\sim 96\text{kJ mol}^{-1}$ and $\sim 140\text{kJ mol}^{-1}$ for di- and tri-vacancies [33], respectively. While the formation energies for these multi-vacancies is lower than the sum of mono-vacancies, recall that the probability of existence of vacancies follows the Boltzmann distribution. The implication is that the equilibrium probability of a di-vacancy at 300K is 10^{-8} lower than that of a single vacancy and this probability ratio drops to 10^{-16} for a tri-vacancy. The conclusion is that energetic barriers make vacancy coalescence a highly unlikely event.

An important reason for why the vacancy diffusion models miss the key physics of drift is that the models either write empirical equations [20,21,23,29] or propose field equations [30] without deriving consistent kinematics and thermodynamics of the assumed processes. The present study aims to address this deficiency. We develop a thermodynamically consistent variational principle and the governing equations for vacancy flux in a monovalent metal electrode that is being stripped into a solid electrolyte. We make use of the Onsager [34,35] formalism via a one-dimensional (1D) treatment in which the only component of velocity of both metal atoms and vacancies is orthogonal to the planar interface between metal anode and solid electrolyte. This approach thus precludes creep which has been investigated in other studies [24–28] and therefore also the formation of macroscopic voids and the associated three-dimensional motion of both metal atoms and vacancies. However, this 1D study is simple and insightful (in line with other 1D studies, e.g., [36]) and will clarify the role of vacancy diffusion which is the primary focus of this paper. Specifically, we use the 1D model to (i) illustrate the important consequences of neglecting the electrode drift in the vacancy diffusion analyses reported in the literature and (ii) explain the methodology to construct a thermodynamically consistent framework for vacancy diffusion within a stripping electrode.

2. Variational framework for stripping with vacancy diffusion

We consider the 1D stripping of Li through a solid electrolyte from a Li electrode; the half-cell is sketched in Fig. 3. The half-cell comprises a Li electrode of thickness H , a current collector adhered to the electrode and a portion of the electrolyte. The origin of our fixed co-ordinate system is located at the electrode/electrolyte interface as shown in Fig. 3. To analyse the stripping process, consider a system comprising the entire Li electrode of thickness H , a portion of the electrolyte of infinitesimal thickness, and absent the copper current collector. The electrode is taken to be a perfect electron conductor maintained at an electric potential ϕ_p and the electric potential of the electrolyte immediately in contact with the electrode is ϕ_e . Allow for vacancy diffusion within the electrode but neglect creep deformation in this 1D context (incompressible creep deformation cannot be modelled realistically in 1D). Furthermore, to simplify the analysis, assume that the electrode has a rigid atomic lattice which implies that: (i) we are neglecting elastic deformation of the Li and (ii) the volumes of each vacancy and of each Li atom are equal. The rigid lattice assumption is justified by recalling that the strength of Li metal at room temperature is $\sim 1\text{MPa}$ [37]. Consequently, the elastic (or lattice) strain is on the order of 0.2×10^{-3} and thus over a $10\mu\text{m}$ thick electrode the lattice deformation will not exceed

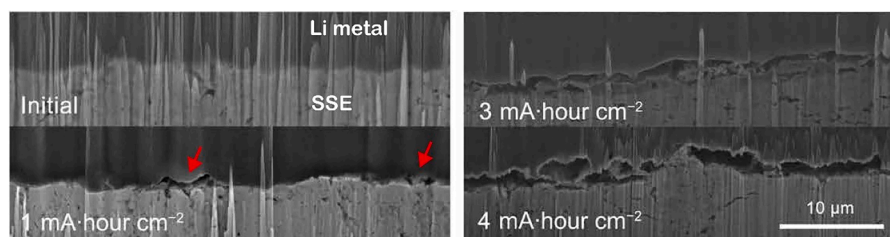


Fig. 1. Cross-sectional SEM images of the Li metal electrode and Lithium Phosphorous Sulphide (LPS) solid electrolyte interface during continuous Li stripping showing void initiation (red arrows) and growth at a stripping current of 0.5mA cm^{-2} . Adapted from [23].

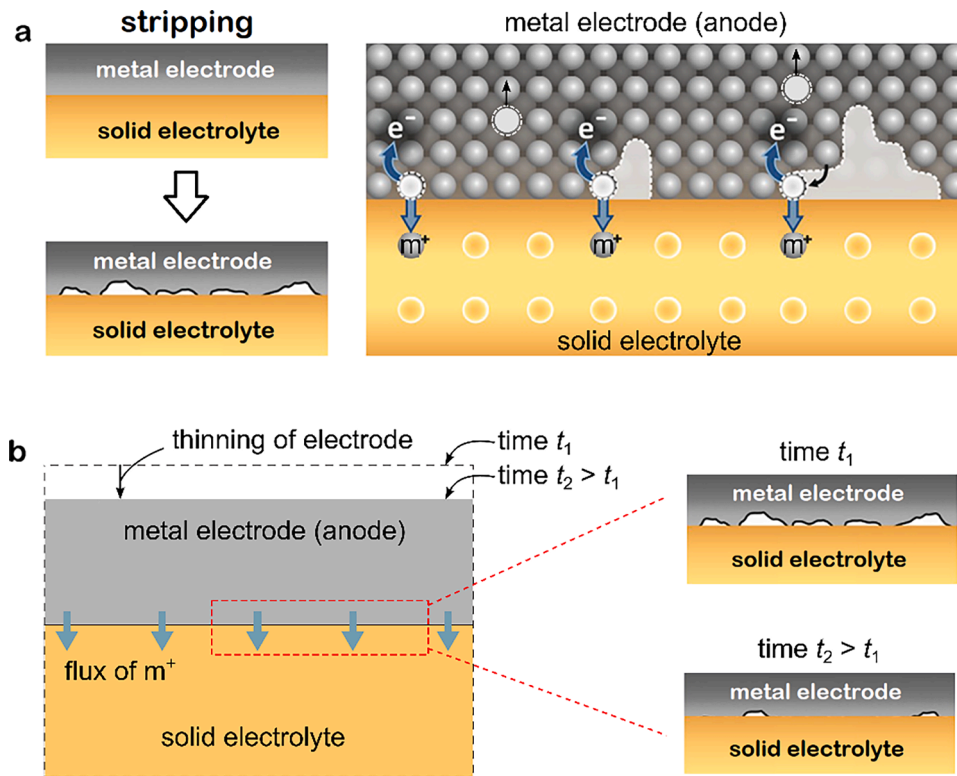


Fig. 2. (a) Sketch illustrating the mechanism of void formation at the electrode/electrolyte interface by vacancy generation and coalescence during stripping of metal ions (m^+). Vacancies are generated at the interface during stripping and their diffusion away from the interface is slower than the rate at which metal atoms is stripped. (b) Vacancies generated by stripping at the electrode/electrolyte interface are annihilated by drift (thinning) of the electrode.

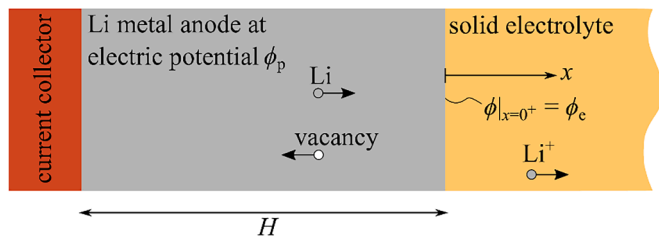


Fig. 3. Sketch of the 1D stripping problem analysed where the origin of the coordinate system is fixed at the electrode/electrolyte interface, i.e., at $x = 0$. The current collector is adhered to the electrode at $x = -H$ and the electrolyte is located at $x > 0$.

$\sim 2\text{nm}$. We thus simplify the model development using the rigid lattice assumption given that this assumption has little influence on vacancy diffusion upon stripping of the electrode.

Write ρ_L as the molar density per unit volume of lattice sites in the electrode and μ_0 as the reference molar chemical potential of Li. Then, the Helmholtz free-energy per unit volume of the electro-neutral electrode, when a number fraction θ of vacant lattice sites is present at a temperature T , is

$$a = \rho_L(1 - \theta)\mu_0 + \theta\rho_L h_v + \rho_L RT[\theta \ln \theta + (1 - \theta) \ln(1 - \theta)], \quad (1)$$

where h_v is the enthalpy of vacancy formation and R is the universal gas constant. In (1), we have neglected the possibility of vacancy coalescence given the high energy barrier for such an event as discussed in the introduction. The number fraction of vacant sites $\theta(x, t)$ is a function of the spatial position x (measured with respect to the electrode/electrolyte interface) within the electrode and time t . We proceed to develop a formulation to predict the spatio-temporal evolution of θ .

The time rate of change of free-energy follows from (1) as

$$\dot{a} = \rho_L \dot{\theta} \left[(h_v - \mu_0) + RT \ln \frac{\theta}{1 - \theta} \right], \quad (2)$$

since we have assumed a rigid lattice such that $\dot{\rho}_L = 0$. We wish to calculate the rate of change of potential energy $\dot{\Pi}$ of the system which includes the relevant fluxes across the boundaries of the system. Upon denoting j_D as the diffusive flux of vacancies through the electrode (with respect to the reference frame fixed to the lattice), the flux j_m of Li metal atoms through a spatially fixed location x is given by

$$j_m = (1 - \theta)\rho_L v - j_D, \quad (3)$$

where v is the spatially constant velocity of the lattice as we have assumed a rigid lattice. Then, conservation of the Li atoms implies that

$$\rho_L \dot{\theta} = \frac{dj_m}{dx} = - \left(\rho_L v \frac{\partial \theta}{\partial x} + \frac{dj_D}{dx} \right). \quad (4)$$

Now recall that during stripping there is a flux of Li^+ ions out of the system into the electrolyte as well as a corresponding flux j_{e^-} of electrons out of the system into the current collector. The rate of change of potential energy $\dot{\Pi}$ of the system then follows as

$$\dot{\Pi} = \frac{\partial}{\partial t} \left(\int_{-H}^0 a \, dx \right) + (\mu_e + F\phi_e + \mu_{e^-}) j_m|_{x=0}, \quad (5)$$

where μ_e and $\mu_{e^-} = -F\phi_p$ are the chemical potential of the Li^+ ions in the electrolyte immediately in contact with the electrode and the chemical potential of the electrons in the electrode, respectively, and F denotes the Faraday constant. In deriving (5), we have used the fact that the oxidation reaction at the electrode/electrolyte interface generates an electron flux with electroneutrality requiring that the magnitude of the electron flux into the current collector equals the flux of Li^+ ions into the electrolyte. Now make use of the Leibniz integral rule to re-write (5) as

$$\dot{\Pi} = \int_{-H}^0 \dot{a} dx + a|_{x=-H} \dot{H} + [\mu_e + F(\phi_e - \phi_p)] j_m|_{x=0}, \quad (6)$$

where the change in the electrode thickness is related to the metal flux via the conservation statement

$$\dot{H} = -\frac{1}{(1 - \theta|_{x=-H})\rho_L} j_m|_{x=-H}. \quad (7)$$

We shall employ the Onsager [34,35] formalism to calculate the kinetic path that this non-equilibrium system acquires. The Onsager formalism requires that the kinetic path is such that arbitrary variations in rate kinematic degrees of freedom give a rate of change of potential energy that is balanced by the variation in the dissipation rate. Assume a dissipation potential Φ that comprises two sources of dissipation: (i) dissipation associated with the flux of Li^+ across the electrode/electrolyte interface and (ii) dissipation due to vacancy diffusion in the Li electrode. Following Shishvan et al. [24], we define an electrode/electrolyte interface dissipation potential $\Phi_I \equiv (Fj_m|_{x=0})^2 Z/2$ where Z is the interfacial resistance. This dissipation potential is appropriate for linearised Butler-Volmer kinetics. The dissipation potential associated with vacancy diffusion is given by

$$\Phi_D \equiv \frac{1}{2\rho_L M} \int_{-H}^0 \frac{j_D^2}{\theta} dx, \quad (8)$$

where M is the mobility of vacancies which is related to the vacancy diffusion co-efficient D_v via the Einstein relation $D_v \equiv MRT$.

To proceed with the Onsager formulation, introduce an augmented potential

$$\Psi(j_m, v) \equiv \dot{\Pi} + \Phi_D + \Phi_I, \quad (9)$$

such that the kinematic solution is required to satisfy $\delta\Psi = 0$. Now consider the variation of each term on the right-hand side of (9) in turn. Upon substitution from (2), (4) and (7) into (6) we have

$$\begin{aligned} \delta\dot{\Pi} = & \int_{-H}^0 \left[(h_v - \mu_0) + RT \ln \frac{\theta}{1-\theta} \right] \frac{\partial \delta j_m}{\partial x} dx \\ & + [\mu_e + F(\phi_e - \phi_p)] \delta j_m|_{x=0} - \frac{a|_{x=-H}}{(1 - \theta|_{x=-H})\rho_L} \delta j_m|_{x=-H}. \end{aligned} \quad (10)$$

Integrate the above expression by parts and introduce an overpotential $\eta \equiv \phi_p - (\phi_e + \mathcal{U})$ where the open circuit potential is $\mathcal{U} \equiv (\mu_e - \mu_0)/F$; then, (10) reduces to

$$\begin{aligned} \delta\dot{\Pi} = & -RT \int_{-H}^0 \left(\frac{1}{\theta} + \frac{1}{1-\theta} \right) \frac{\partial \theta}{\partial x} \delta j_m dx + \left(h_v + RT \ln \frac{\theta|_{x=0}}{1-\theta|_{x=0}} - F\eta \right) \delta j_m|_{x=0} \\ & + \left[\mu_0 - h_v - RT \ln \frac{\theta|_{x=-H}}{1-\theta|_{x=-H}} - \frac{a|_{x=-H}}{(1-\theta|_{x=-H})\rho_L} \right] \delta j_m|_{x=-H}. \end{aligned} \quad (11)$$

Now consider the variation of the dissipation potential which follows from the definitions of Φ_I and Φ_D as

$$\delta\Phi_I + \delta\Phi_D = F^2 Z j_m|_{x=0} \delta j_m|_{x=0} + \frac{1}{\rho_L M} \int_{-H}^0 \frac{j_D \delta j_D}{\theta} dx, \quad (12)$$

where from (3) $\delta j_D = -\delta j_m + (1 - \theta)\rho_L \delta v$. Upon combining (11) and (12) and setting $\delta\Psi = 0$, we obtain

$$\begin{aligned} & - \int_{-H}^0 \frac{1}{\theta} \left(\frac{RT}{1-\theta} \frac{\partial \theta}{\partial x} + \frac{j_D}{\rho_L M} \right) \delta j_m dx + \frac{\delta v}{M} \int_{-H}^0 j_D \frac{1-\theta}{\theta} dx \\ & - \left[\frac{1}{1-\theta|_{x=-H}} (h_v + RT \ln \theta|_{x=-H}) \right] \delta j_m|_{x=-H} \\ & + \left[h_v + RT \ln \frac{\theta|_{x=0}}{1-\theta|_{x=0}} - F\eta + F^2 Z j_m|_{x=0} \right] \delta j_m|_{x=0} = 0. \end{aligned} \quad (13)$$

This completes the general variational statement. Since δj_m is arbitrary throughout the domain, the first term in (13) implies that

$$j_D = -\frac{\rho_L D_v}{1-\theta} \frac{\partial \theta}{\partial x}, \quad (14)$$

where $D_v = MRT$ and (14) is the flux law for vacancies. The combination of (14) and (4) gives the overall governing differential equation as

$$\dot{\theta} = - \left[v \frac{\partial \theta}{\partial x} - D_v \frac{\partial}{\partial x} \left(\frac{1}{1-\theta} \frac{\partial \theta}{\partial x} \right) \right], \quad (15)$$

which is the usual 1D differential equation for diffusion with drift. Note that the drift velocity v will be an outcome of the boundary conditions as we shall subsequently discuss. However, the initial conditions to (15) are straightforward to specify. It is natural to assume that the electrode prior to imposition of a stripping current i_{cell} or an overpotential η is at equilibrium. In the absence of an imposed pressure, the Gibbs free-energy of the electrode comprising N_{Li} moles of Li and N_L lattice sites is given by (1) as

$$\begin{aligned} \mathcal{G} = & N_L \mu_0 + (N_L - N_{\text{Li}})(h_v - \mu_0) \\ & + N_L RT \left[\frac{N_{\text{Li}}}{N_L} \ln \frac{N_{\text{Li}}}{N_L} + \left(1 - \frac{N_{\text{Li}}}{N_L} \right) \ln \left(1 - \frac{N_{\text{Li}}}{N_L} \right) \right], \end{aligned} \quad (16)$$

where $\theta = 1 - N_{\text{Li}}/N_L$ is used to rearrange (1). Now consider an isobaric-isothermal ensemble (NpT -ensemble) where the only particles are Li atoms (i.e., lattice sites and Li atoms are the two species in the system). Then, within the context of the NpT -ensemble, the electrode attains equilibrium with a vacancy reservoir at fixed N_{Li} by changing the number of lattice sites. Thus, at equilibrium

$$\left. \frac{\partial \mathcal{G}}{\partial N_L} \right|_{N_{\text{Li}}, T} = 0, \quad (17)$$

and it follows that the number fraction of vacant sites is $\theta = \exp[-h_v/(RT)]$. This gives the initial condition for (15) as $\theta = \theta_0 = \exp[-h_v/(RT)] \forall x$, along with the stripping current or overpotential imposed at time $t = 0$.

2.1. Constraint imposed by the current collector

The current collector that is adhered to the electrode at $x = -H$ restricts the flux of vacancies across the electrode/current collector interface implying that $j_D|_{x=-H} = 0$. It immediately follows from (3) that

$$v = \frac{j_m|_{x=-H}}{\rho_L (1 - \theta|_{x=-H})}. \quad (18)$$

In the limit of a rigid lattice assumed here, v is spatially uniform and thus (18) implies that v is no longer an independent kinetic variable and we can rewrite (13) as

$$\begin{aligned} & - \int_{-H}^0 \frac{1}{\theta} \left(\frac{RT}{1-\theta} \frac{\partial \theta}{\partial x} + \frac{j_D}{\rho_L M} \right) \delta j_m dx + \frac{\delta j_m|_{x=-H}}{\rho_L M (1 - \theta|_{x=-H})} \int_{-H}^0 j_D \frac{1-\theta}{\theta} dx \\ & - \left[\frac{1}{1-\theta|_{x=-H}} (h_v + RT \ln \theta|_{x=-H}) \right] \delta j_m|_{x=-H} \\ & + \left[h_v + RT \ln \frac{\theta|_{x=0}}{1-\theta|_{x=0}} - F\eta + F^2 Z j_m|_{x=0} \right] \delta j_m|_{x=0} = 0. \end{aligned} \quad (19)$$

Upon substituting for j_D from (14) and integration of the 2nd integral, it follows that

$$\begin{aligned}
& - \int_{-H}^0 \frac{1}{\theta} \left(\frac{RT}{1-\theta} \frac{\partial \theta}{\partial x} + \frac{j_D}{\rho_L M} \right) \delta j_m dx \\
& - \left[\frac{1}{1-\theta|_{x=-H}} (h_v + RT \ln \theta|_{x=0}) \right] \delta j_m|_{x=-H} \\
& + \left[h_v + RT \ln \frac{\theta|_{x=0}}{1-\theta|_{x=0}} - F\eta + F^2 Z j_m|_{x=0} \right] \delta j_m|_{x=0} = 0.
\end{aligned} \quad (20)$$

This completes the variational statement for the case of the adhered current collector, and we can now solve (15) by making use of boundary conditions that satisfy (20).

3. Solutions for 1D stripping of the electrode

Boundary conditions for (15) must be chosen in accordance with (20). Consider two limiting cases: (i) stripping with no mechanical constraint imposed on the current collector and (ii) stripping with the current collector mechanically constrained to be fixed in space with respect to the electrode/electrolyte interface, i.e., for a spatially fixed electrolyte, the current collector is also spatially fixed. The boundary condition (ii) is often imposed in the literature [23,29,30] although this is due to a misinterpretation of the kinematics as we shall subsequently discuss.

3.1. Free current collector (allowing for a thinning of the electrode)

Consider the case when no mechanical constraint is imposed on the current collector such that it is allowed to move freely, i.e., \dot{H} is not specified and is an outcome of the solution. Thus, $\delta j_m|_{x=-H}$ is arbitrary and the 2nd term in (20) then implies that

$$\theta|_{x=0} = \exp\left(\frac{h_v}{RT}\right). \quad (21)$$

Similarly, $\delta j_m|_{x=0}$ is also arbitrary and then, upon substituting for $\theta|_{x=0}$ from (21) into the 3rd term in (20), the stripping current $i_{\text{cell}} \equiv F j_m|_{x=0}$ is related to the overpotential such that

$$i_{\text{cell}} = \frac{\eta}{Z} + \frac{RT}{FZ} \ln \left[1 - \exp\left(-\frac{h_v}{RT}\right) \right]. \quad (22)$$

The conditions (21) and (22) along with the initial condition $\theta = \theta_0 = \exp[-h_v/(RT)] \forall x$ admit a trivial solution to (15) such that $j_D = \dot{\theta} = \partial\theta/\partial x = 0$ and (3) delivers

$$v = -\dot{H} = \frac{i_{\text{cell}}}{F\rho_L(1-\theta_0)} \approx \frac{i_{\text{cell}}}{F\rho_L}. \quad (23)$$

The approximate solution in (23) holds in the practical case for Li at room temperature where $\theta_0 \ll 1$. Eq. (23) implies that there is no vacancy diffusion, the lattice undergoes rigid body drift and the electrode thins to accommodate the stripping current. Thus, no void growth is expected under these circumstances.

3.2. Mechanically constrained current collector (which prevents thinning of the electrode)

Now consider the other extreme condition where the current collector is held fixed so that $\dot{H} = j_m|_{x=-H} = 0$. Given that $j_D|_{x=-H} = 0$, it follows from (3) that $v = 0$ and the governing differential Eq. (15) reduces to a standard diffusion equation

$$\dot{\theta} = D_v \frac{\partial}{\partial x} \left(\frac{1}{1-\theta} \frac{\partial \theta}{\partial x} \right). \quad (24)$$

For an imposed stripping current, $i_{\text{cell}} \equiv F j_m|_{x=0}$, the boundary conditions for (24) are the Neumann and Robin boundary conditions

$$\frac{\partial \theta}{\partial x} = \begin{cases} 0 & x = -H, \\ \frac{i_{\text{cell}}(1-\theta)}{\rho_L F D_v} & x = 0, \end{cases} \quad (25)$$

where the Robin boundary condition is obtained by substituting for j_D from (14) into (3). The corresponding overpotential follows from recognising that the flux variation $\delta j_m|_{x=0}$ is arbitrary and thus the 3rd term of (20) gives

$$\eta = i_{\text{cell}} Z + \frac{1}{F} \left(h_v + RT \ln \frac{\theta|_{x=0}}{1-\theta|_{x=0}} \right). \quad (26)$$

For this case of the mechanically constrained current collector, the governing equation (24) does not admit a trivial solution and we proceed to report numerical solutions.

3.2.1. Numerical predictions

We restrict attention to the case of loading where a fixed stripping current i_{cell} is imposed and the corresponding overpotential $\eta(t)$ is an outcome of the solution via (26). The problem thus reduces to solving the diffusion equation (24) with initial conditions $\theta = \theta_0 \forall x$ and boundary conditions (25). All results are presented at room temperature $T = 295\text{K}$ and for well-established Li properties, viz., $\rho_L = 76, 300\text{mol m}^{-3}$, $h_v = 50\text{kJ mol}^{-1}$ [32] and $D_v = 10^{-14} \text{m}^2\text{s}^{-1}$ [20,23,38–40]. The calculations are reported for an electrode of thickness $H = 1\text{mm}$ to simulate a thick electrode where the influence of the current collector is small.

First, consider the case of a prescribed stripping current $i_{\text{cell}} = 1\text{mA cm}^{-2}$. Predictions of the spatio-temporal distributions of θ are included in Fig. 4a. Vacancies are nucleated at the electrode/electrolyte interface as Li^+ ions are stripped, and these vacancies diffuse into the bulk of the electrode. The vacancy fraction θ rises at the interface $x = 0$ such that, after 1.2hrs, the electrode is a porous solid over $20\mu\text{m}$ from the electrode/electrolyte interface. It is likely that the vacancy fraction at the electrode/electrolyte interface governs cell failure and therefore we include predictions of the temporal variation of $\theta|_{x=0}$ for selected stripping currents in the range $0.5\text{mA cm}^{-2} \leq i_{\text{cell}} \leq 1\text{mA cm}^{-2}$ in Fig. 4b. For all values of imposed current density, $\theta|_{x=0}$ rises rapidly and then slowly attains the limiting value of $\theta|_{x=0} = 1$.

Recall that cell failure in experiments is defined by a precipitous rise in the cell voltage or, equally, the overpotential rather than a critical value of electrode porosity. To make this connection, we include in Fig. 5a temporal predictions of η using (26) for selected stripping currents in the range $0.5\text{mA cm}^{-2} \leq i_{\text{cell}} \leq 1\text{mA cm}^{-2}$ and $Z = 5\Omega\text{cm}^2$, representative of an interface between Li and the garnet electrolyte LLZO ($\text{Li}_7\text{La}_3\text{Zr}_2\text{O}_{12}$) [41]. However, unlike observations, the model predicts a sudden rise in η very early in the stripping history from the initial value $\approx i_{\text{cell}} Z$ to nearly ~ 100 times this value (also see the inset of Fig. 5a). This sudden increase is followed by a much more gradual increase. In experiments, there is a gradual increase in η from the start of stripping until cell failure, defined by a sudden rise in η . This discrepancy between predictions and observations can be understood as follows. From the onset of stripping the vacancy fraction $\theta|_{x=0}$ at the interface rises (Fig. 4b). The overpotential is directly related to $\theta|_{x=0}$ via (26) and comprises two terms: $i_{\text{cell}} Z$ and a term associated with the vacancy fraction. At $\theta = \theta_0$, the contribution from the vacancy fraction term is negligible and $\eta \approx i_{\text{cell}} Z$ but as θ increases this second term becomes the dominant contribution. We observe from Fig. 4b that for the stripping current of $i_{\text{cell}} = 1\text{mA cm}^{-2}$, $\theta|_{x=0}$ increases from its initial equilibrium value of $\theta_0 \approx 1.4 \times 10^{-9}$ to $\theta = 0.05$ in 10s and it is this large increase in θ that results in the very early rise in η as seen in Fig. 5a. Given that only a very gradual initial increase in η is measured in experiments, it is unlikely that vacancy growth is initially rapid, as predicted here by the diffusion analysis when the current collector is mechanically constrained.

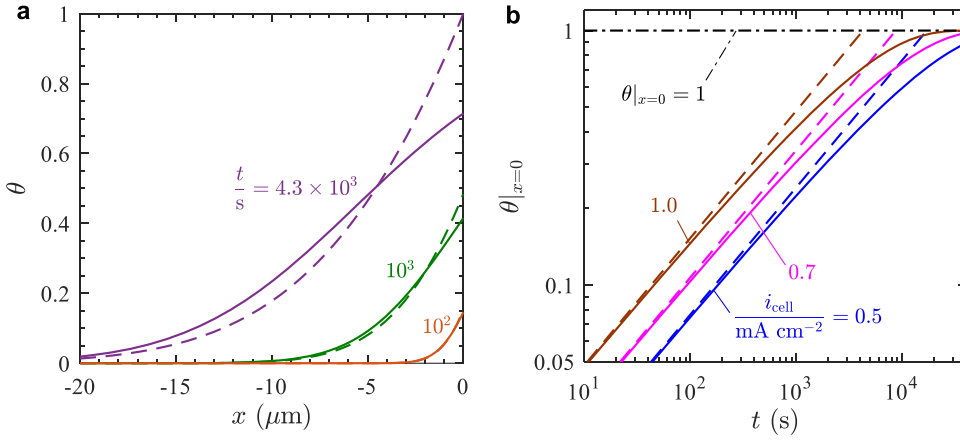


Fig. 4. Stripping with the mechanically constrained current collector. (a) Spatio-temporal distribution of the vacancy fraction, θ , for $i_{\text{cell}} = 1 \text{ mA cm}^{-2}$. (b) Temporal variations of $\theta|_{x=0}$ for selected stripping currents in the range $0.5 \text{ mA cm}^{-2} \leq i_{\text{cell}} \leq 1 \text{ mA cm}^{-2}$. Analytical predictions (27) and (28) are included in (a) and (b), respectively, as dashed lines. Eq. (28) and $\theta|_{x=0} = 1$ are two asymptotes for the full numerical predictions in (b). Time $t = 0$ corresponds to the instant that stripping is initiated.

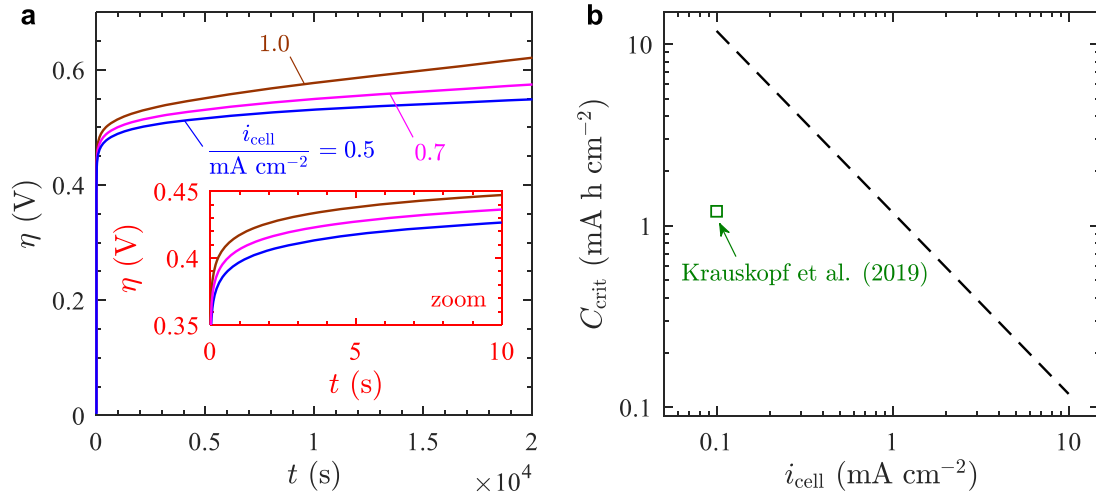


Fig. 5. Stripping with the mechanically constrained current collector. (a) Temporal variation of the interface overpotential η for selected stripping currents in the range $0.5 \text{ mA cm}^{-2} \leq i_{\text{cell}} \leq 1 \text{ mA cm}^{-2}$ and interface resistance $Z = 5 \Omega \text{ cm}^2$. The inset shows the early time history over the range $0 < t < 10 \text{ s}$. (b) The prediction (30) of C_{crit} over a wide range $0.1 \leq i_{\text{cell}} (\text{mA cm}^{-2}) \leq 10$. The measurement of Krauskopf et al. [20] is included.

While there seem to be some clear discrepancies between observations and predictions of this analysis, the model nevertheless predicts a growth in the vacancy fraction at the interface and is therefore capable of providing an estimate of the time for failure of the cell and the corresponding critical cell capacity. However, it is difficult to unambiguously define failure from these numerical predictions as the expression (1) for the free-energy implies that $\theta|_{x=0}$ tends to unity but does not attain unity within finite time. We thus adopt a simpler approach which is also predicated on the recognition that the free-energy expression (1) loses accuracy at large vacancy content when the Li electrode begins to resemble a foamed metal rather than a solid metal electrode. Observe that the diffusion equation (24) reduces to linearity for $\theta \ll 1$. Then, taking the limit $\theta \rightarrow 0$ in (24) and (25), we find a simple analytical solution for $\theta(x, t)$ as

$$\theta(x, t) = \theta_0 + \frac{2i_{\text{cell}}}{\rho_{\text{L}} F D_{\text{v}}} \left[\frac{\sqrt{D_{\text{v}} t}}{\sqrt{\pi}} \exp\left(-\frac{x^2}{4D_{\text{v}} t}\right) + \frac{x}{2} \operatorname{erfc}\left(\frac{|x|}{2\sqrt{D_{\text{v}} t}}\right) \right], \quad (27)$$

in the limit of a thick electrode where $H \rightarrow \infty$. Predictions of (27) included in Fig. 4a agree remarkably well with the full non-linear predictions in the low θ range where (27) is anticipated to be accurate. Of primary concern is the temporal evolution of $\theta|_{x=0}$ and this follows from (27) as

$$\theta|_{x=0} = \theta_0 + \frac{2i_{\text{cell}}}{\rho_{\text{L}} F} \frac{\sqrt{t}}{\sqrt{D_{\text{v}} \pi}}. \quad (28)$$

The analytical predictions (28) are included in Fig. 4b and we observe that (28) and $\theta|_{x=0} = 1$ represent the two asymptotes to the full numerical prediction. This immediately suggests that an appropriate definition of the failure time is given by the intersection of these two asymptotes, viz., the failure time t_{f} is obtained by setting $\theta|_{x=0} = 1$ in (28) so that

$$t_{\text{f}} = \pi D_{\text{v}} \left[\frac{(1 - \theta_0) \rho_{\text{L}} F}{2i_{\text{cell}}} \right]^2. \quad (29)$$

The capacity C_{crit} of the cell at cell failure is then given by

$$C_{\text{crit}} \equiv i_{\text{cell}} t_{\text{f}} = \frac{\pi D_{\text{v}}}{4i_{\text{cell}}} [(1 - \theta_0) \rho_{\text{L}} F]^2. \quad (30)$$

The critical capacity C_{crit} from (30) over a wide range $0.1 \text{ mA cm}^{-2} \leq i_{\text{cell}} \leq 10 \text{ mA cm}^{-2}$ is included in Fig. 5b. In line with measurements, the predicted value of C_{crit} reduces with increasing i_{cell} . There are very limited data available for cell failure in the absence of stack pressure as considered in our current 1D study. Krauskopf et al. [20] reported $C_{\text{crit}} \approx 1.2 \text{ mA h cm}^{-2}$ for stripping at $i_{\text{cell}} = 0.1 \text{ mA cm}^{-2}$ for a Li/LLZO/Li symmetric cell and this measurement is included in Fig. 5b where predictions suggest a value of $C_{\text{crit}} \approx 10 \text{ mA h cm}^{-2}$. Given that the

prediction is from a simple 1D calculation with no interface impurities or other heterogeneities, we might be inclined to disregard this discrepancy between theory and experiment and conclude that this model represents the actual stripping failure mechanism. Here, we shall argue otherwise. Although some qualitative features of these results are in line with observations (and other features such as the $\eta(t)$ predictions that are divergent from observations), a model that assumes full mechanical constraint of the current collector is in direct contradiction to the actual experimental setup as reported in the literature [23,29,30].

4. Concluding discussion

The formulation detailed in Section 2 demonstrates that, in the absence of creep, there are two kinematic variables in the problem: (i) flux of Li (or vacancies) and (ii) the lattice drift velocity which in general is a field variable that can vary with position but reduces to a rigid body velocity in the limit of the non-deformable lattice assumed here. A thermodynamically consistent formulation, as presented here, implies that there exist work conjugates to these two kinematic variables, viz., the chemical potential of the Li (or vacancies) is the conjugate to the flux of Li (or vacancies), while a traction is the work-conjugate to the velocity of the rigid lattice.

In the presence of an adhered current collector, it is reasonable to assume that the vacancy flux relative to the lattice vanishes at the current collector, as assumed in the literature [23,29,30]. However, these studies directly relate the Li flux to the vacancy flux via the relation $j_m = -j_D$. Comparing with (3), it is clear that the modelling studies in the literature [23,29,30] implicitly assume a vanishing drift velocity of the lattice. Therefore, the analyses in the literature reduce to the mechanically constrained current collector analysis as described in Section 3.2 and predict that the electrode does not thin. In practice, (with an imposed stack pressure present or absent) the stripping Li electrode thins as the Li is transported across the electrolyte into the plating electrode. If the electrode were prevented from thinning in an experiment, then a tensile traction (which is conjugated to the lattice drift velocity) would develop on the current collector.¹ Such a constraint is never imposed in any experiment or practical cell.

In contrast, in our analysis, we have correctly recognised that the Li flux and drift velocity are two independent variables. We can therefore decouple these variables and allow the electrode to thin while still ensuring that the vacancy flux vanishes at the current collector. This corresponds to our free current collector boundary condition of Section 3.1 where the analysis predicts that 1D stripping occurs with no vacancy diffusion and in fact $\theta = \theta_0 \forall (x, t)$ such that stripping occurs purely by thinning of the electrode due to drift of the lattice. The 1D analysis gives an unambiguous prediction that stripping does not result in void/vacancy formation at the electrode/electrolyte interface and consequently no cell failure occurs.

Note that lattice drift is naturally included in Eulerian [24] or arbitrary Lagrangian/Eulerian [26] analyses. On the other hand, Lagrangian analyses are commonly used in the literature and drift has largely been neglected in those treatments, whereas it needs to be explicitly accounted for, as described in our study. A recent investigation [42] attempts to include drift in a Lagrangian analysis wherein a drift velocity is explicitly enforced as a boundary condition rather than being allowed to emerge naturally. The approach in [42] results in over-defined boundary conditions with associated issues of numerical ill-posedness.

In summary, both versions of the 1D analyses presented here cannot

¹ The analysis of Section 2 implicitly has such a traction which is conjugated to the drift velocity v . However, the rigid lattice assumption employed here (which neglects elasticity) implies that the magnitude of that traction is not predicted. The formulation presented here can be readily extended to a non-rigid lattice including elasticity to predict the tensile traction required to mechanically constrain the current collector.

explain the observation of cell failure at the stripping Li electrode due to the formation of voids, albeit for different reasons. The mechanically constrained current collector boundary condition predicts vacancy growth at the electrode/electrolyte interface, suggesting that it predicts cell failure akin to observations. However, this boundary condition, which prevents thinning of the electrode, is at odds with experimental protocol and observations. On the other hand, the free current collector boundary condition accurately captures the experimental boundary conditions but unlike observations it predicts that voids will not form at the electrode/electrolyte interface by vacancy coalescence. There are numerous reasons for this discrepancy including: (i) imperfections such as impurity particles [24,26] and surface roughness [27] are required at the interface to initiate void growth; and/or (ii) creep of the electrode results in a break-down of Butler-Volmer kinetics [24]. While reasons for the observed void formation at the electrode/electrolyte interface remain an open research question, we have demonstrated here that the drift of the electrode that is inherent in the thinning of the stripping electrode has a strong tendency to close voids.

CRedit authorship contribution statement

S.S. Shishvan: Methodology, Software, Validation, Formal analysis, Writing – review & editing. **N.A. Fleck:** Validation, Writing – review & editing. **R.M. McMeeking:** Conceptualization, Validation, Writing – original draft. **V.S. Deshpande:** Conceptualization, Validation, Writing – original draft.

Declaration of Competing Interest

The authors declare that they have no known competing financial interests or personal relationships that could have appeared to influence the work reported in this paper.

Data availability

No data was used for the research described in the article.

Acknowledgements

NAF is grateful for funding from the Faraday Institution for Degradation II project [grant number FIRG024].

References

- [1] K. Takada, Progress and prospective of solid-state lithium batteries, *Acta Mater.* 61 (2013) 759–770.
- [2] M.J. Wang, E. Kazyak, N.P. Dasgupta, J. Sakamoto, Transitioning solid-state batteries from lab to market: linking electro-chemo-mechanics with practical considerations, *Joule* 16 (2021) 1371–1390.
- [3] J.L. Barton, J.O'M. Bockris, The electrolytic growth of dendrites from ionic solutions, *Proc. R. Soc. A* 268 (1962) 485–505.
- [4] J.W. Diggle, A.R. Despic, J.O'M. Bockris, The mechanism of dendritic electrocrystallization of zinc, *J. Electrochem. Soc.* 116 (1969) 1503–1514.
- [5] C. Monroe, J. Newman, The effect of interfacial deformation on electrodeposition kinetics, *J. Electrochem. Soc.* 151 (6) (2004) A880–A886.
- [6] E. Kazyak, R. Garcia-Mendez, W.S. LePage, A. Sharaifi, A.L. Davis, A.J. Sanchez, K. H. Chen, C. Haslam, J. Sakamoto, N.P. Dasgupta, Li penetration in ceramic solid electrolytes: operando microscopy analysis of morphology, propagation, and reversibility, *Matter* 2 (4) (2020) 1025–1048.
- [7] M. Rosso, C. Brissot, A. Teyssot, M. Doll, L. Sannier, J.M. Tarascon, R. Bouchet, S. Lescaud, Dendrite short-circuit and fuse effect on Li/polymer/Li cells, *Electrochim. Acta* 51 (2006) 5334.
- [8] L. Porz, T. Swamy, B.W. Sheldon, D. Rettenwander, T. Frömling, H.L. Thaman, S. Berendts, R. Uecker, W.C. Carter, Y.M. Chiang, Mechanism of lithium metal penetration through inorganic solid electrolytes, *Adv. Energy Mater.* 7 (20) (2017), 1701003.
- [9] J. Kasemchainen, S. Zekoll, D. Spencer Jolly, Z. Ning, G.O. Hartley, J. Marrow, P. G. Bruce, Critical stripping current leads to dendrite formation on plating in lithium anode solid electrolyte cells, *Nat. Mater.* 18 (2019) 1105–1111.

- [10] D.S. Jolly, Z. Ning, J.E. Darnbrough, J. Kasemchainen, G.O. Hartley, P. Adamson, D.E. Armstrong, J. Marrow, P.G. Bruce, Sodium/Na β'' alumina interface: effect of pressure on voids, *ACS Appl. Mater. Interfaces* 12 (2020) 678–685.
- [11] Z. Ning, D. Spencer Jolly, G. Li, R. De Meyere, S.D. Pu, Y. Chen, J. Kasemchainen, J. Ihli, C. Gong, B. Liu, D.L.R. Melvin, A. Bonnin, O. Magdysyuk, P. Adamson, G. O. Hartley, C.W. Monroe, T.J. Marrow, P.G. Bruce, Visualizing plating-induced cracking in lithium-anode solid electrolyte cells, *Nat. Mater.* 20 (2021) 1121–1129.
- [12] R.D. Schmidt, J. Sakamoto, In-situ, non-destructive acoustic characterization of solid-state electrolyte cells, *J. Power Sources* 324 (2016) 126–133.
- [13] A. Sharafi, E. Kazyak, A.L. Davis, S. Yu, T. Thompson, D.J. Siegel, N.P. Dasgupta, J. Sakamoto, Surface chemistry mechanisms of ultra-low interfacial resistance in the solid-state electrolyte $\text{Li}_7\text{La}_3\text{Zr}_2\text{O}_{12}$, *Chem. Mater.* 29 (2017) 7961–7968.
- [14] W. Chang, R. May, M. Wang, G. Thorsteinsson, J. Sakamoto, L. Marbella, D. Steingart, Evolving contact mechanics and microstructure formation dynamics of the lithium metal- $\text{Li}_7\text{La}_3\text{Zr}_2\text{O}_{12}$ interface, *Nat. Commun.* 12 (2021) 6369.
- [15] S. Hao, S.R. Daemi, T.M.M. Heenan, W. Du, C. Tan, M. Storm, C. Rau, D.J.L. Brett, P.R. Shearing, Tracking lithium penetration in solid electrolytes in 3D by in-situ synchrotron X-ray computed tomography, *Nano Energy* 82 (2021), 105744.
- [16] V. Raj, J.J. Bailey, F. Iacoviello, J. Bu, P.S. Grant, D.J.L. Brett, P.R. Shearing, 3D imaging of lithium protrusions in solid-state lithium batteries using X-ray computed tomography, *Adv. Funct. Mater.* 31 (10) (2021), 2007564.
- [17] V. Raj, V. Venturi, V.R. Kankanallu, B. Kuri, V. Viswanathan, N.P.B. Aetukuri, Direct correlation between void formation and lithium dendrite growth on solid-state electrolytes with interlayers, *Nat. Mater.* 21 (9) (2022) 1050–1056.
- [18] S.S. Shishvan, N.A. Fleck, R.M. McMeeking, V.S. Deshpande, Dendrites as climbing dislocations in ceramic electrolytes: initiation of growth, *J. Power Sources* 456 (2020), 227989.
- [19] S.S. Shishvan, N.A. Fleck, R.M. McMeeking, V.S. Deshpande, Growth rate of lithium filaments in ceramic electrolytes, *Acta Mater.* 196 (2020) 444–455.
- [20] T. Krauskopf, H. Hartmann, W.G. Zeier, J. Janek, Towards a fundamental understanding of the lithium metal anode in solid-state batteries – An electrochemo-mechanical study on the garnet-type solid electrolyte $\text{Li}_{6.25}\text{Al}_{0.25}\text{La}_3\text{Zr}_2\text{O}_{12}$, *ACS Appl. Mater. Interfaces* 11 (2019) 14463–14477.
- [21] T. Krauskopf, B. Mogwitz, C. Rosenbach, W.G. Zeier, J. Janek, Diffusion limitation of lithium metal and Li-Mg alloy anodes on LLZO type solid electrolytes as a function of pressure and temperature, *Adv. Eng. Mater.* 9 (2019), 1902568.
- [22] M.J. Wang, R. Choudhury, J. Sakamoto, Characterizing the Li-solid-electrolyte interface dynamics as a function of stack pressure and current density, *Joule* 3 (2019) 2165–2178.
- [23] Y. Lu, C.Z. Zhao, J.K. Hu, S. Sun, H. Yuan, Z.H. Fu, X. Chen, J.Q. Huang, M. Ouyang, Q. Zhang, The void formation behaviors in working solid-state Li metal batteries, *Sci. Adv.* 8 (2022) eadd0510.
- [24] S.S. Shishvan, N.A. Fleck, V.S. Deshpande, The initiation of void growth during stripping Li electrodes in solid electrolyte cells, *J. Power Sources* 488 (2021), 229437.
- [25] U. Roy, N.A. Fleck, V.S. Deshpande, An assessment of the mechanisms for void growth in Li anodes, *Extreme Mech. Lett.* 46 (2021), 101307.
- [26] J.A.B. Agier, S.S. Shishvan, N.A. Fleck, V.S. Deshpande, Void growth within Li electrodes in solid electrolyte cells, *Acta Mater.* 240 (2022), 118303.
- [27] X. Zhang, Q.J. Wang, K.L. Harrison, S.A. Roberts, S.J. Harris, Pressure-driven interface evolution in solid-state lithium metal batteries, *Cell Rep. Phys. Sci.* 1 (2020), 100012.
- [28] Y. Chen, Z. Wang, X. Li, X. Yao, C. Wang, Y. Li, W. Xue, D. Yu, S.Y. Kim, F. Yang, A. Kushima, G. Zhang, H. Huang, N. Wu, Y.W. Mai, J.B. Goodenough, J. Li, Li metal deposition and stripping in a solid-state battery via Coble creep, *Nature* 578 (2020) 251–255.
- [29] H. Yan, K. Tantratrian, K. Ellwood, E.T. Harrison, M. Nichols, X. Cui, L. Chen, How does the creep stress regulate void formation at the lithium-solid electrolyte interface during stripping? *Adv. Energy Mater.* 12 (2022), 21022833.
- [30] Y. Zhao, R. Wang, E. Martinez-Paneda, A phase field electro-chemo-mechanical formulation for predicting void evolution in the Li-electrolyte interface in all-solid-state batteries, *J. Mech. Phys. Solids* 167 (2022), 104999.
- [31] S.S. Shishvan, N.A. Fleck, R.M. McMeeking, V.S. Deshpande, Void growth in metal anodes in solid-state batteries: recent progress and gaps in understanding, *Eur. J. Mech. A/Solids* 100 (2023), 104998.
- [32] H. Schultz, Defect parameters of bcc metals: group-specific trends, *Mater. Sci. Eng. A141* (1991) 149–167.
- [33] K.M. Zhang, Y.N. Wen, K.W. Xu, Atomic simulation of vacancies in BCC metals with MAEAM, *Cent. Eur. J. Phys.* 4 (2006) 418–493.
- [34] L. Onsager, Reciprocal relations in irreversible processes, I, *Phys. Rev.* 37 (1931) 405–426.
- [35] L. Onsager, Reciprocal relations in irreversible processes, II, *Phys. Rev.* 38 (1931) 2265–2279.
- [36] M. Mykhaylov, M. Ganser, M. Klinsmann, F.E. Hildebrand, I. Guz, R. M. McMeeking, An elementary 1-dimensional model for a solid-state lithium-ion battery with a single ion conductor and a lithium metal negative electrode, *J. Mech. Phys. Solids* 123 (2019) 207–221.
- [37] W.S. LePage, Y. Chen, E. Kazyak, K.H. Chen, A.J. Sanchez, A. Poli, E.M. Arruda, M. D. Thouless, N.P. Dasgupta, Lithium mechanics: roles of strain rate and temperature and implications for lithium metal batteries, *J. Electrochem. Soc.* 166 (2019) A89.
- [38] R. Messer, F. Noack, Nuclear magnetic relaxation by self diffusion in solid lithium: τ_1 -frequency dependence, *Appl. Phys.* 6 (1975) 79–88.
- [39] T.R. Jow, C.C. Liang, Interface between solid electrode and solid electrolyte - A study of the Li/LiI (Al_2O_3) solid-electrolyte system, *J. Electrochem. Soc.* 130 (1983) 737–740.
- [40] E. Dologlou, Self-diffusion in solid lithium, *Glass Phys. Chem.* 36 (2010) 570–574.
- [41] A. Sharafi, C.G. Haslam, R.D. Kerns, J. Wolfenstine, J. Sakamoto, Controlling and correlating the effect of grain size with the mechanical and electrochemical properties of $\text{Li}_7\text{La}_3\text{Zr}_2\text{O}_{12}$ solid-state electrolyte, *J. Mater. Chem. A* 5 (2017) 21491.
- [42] J.A. Lewis, S.E. Sandoval, Y. Liu, D.L. Nelson, S.G. Yoon, R. Wang, Y. Zhao, M. Tian, P. Shevchenko, E. Martinez-Paneda, M.T. McDowell, Accelerated short circuiting in anode-free solid-state batteries driven by local lithium depletion, *Adv. Energy Mater.* 13 (2023), 2204186.